Supplementary Information

A Supramolecular Gel Platform for Selective Naked-Eye Recognition of Thorium(IV) Ion

Yanyi He,[a] Xiao-Qi Yu,[b] and Shanshan Yu[† a]

[a] Key Laboratory of Green Chemistry and Technology, Ministry of Education, College of Chemistry, Sichuan University, Chengdu 610064, P.R. China

[b] Asymmetric Synthesis and Chiral Technology Key Laboratory of Sichuan Province, Department of Chemistry, Xihua University, Chengdu 610039, P. R. China

[†] Corresponding author e-mail: yushanshan@scu.edu.cn (S.Yu).

Table of Contents

1. Synthesis of BINAB

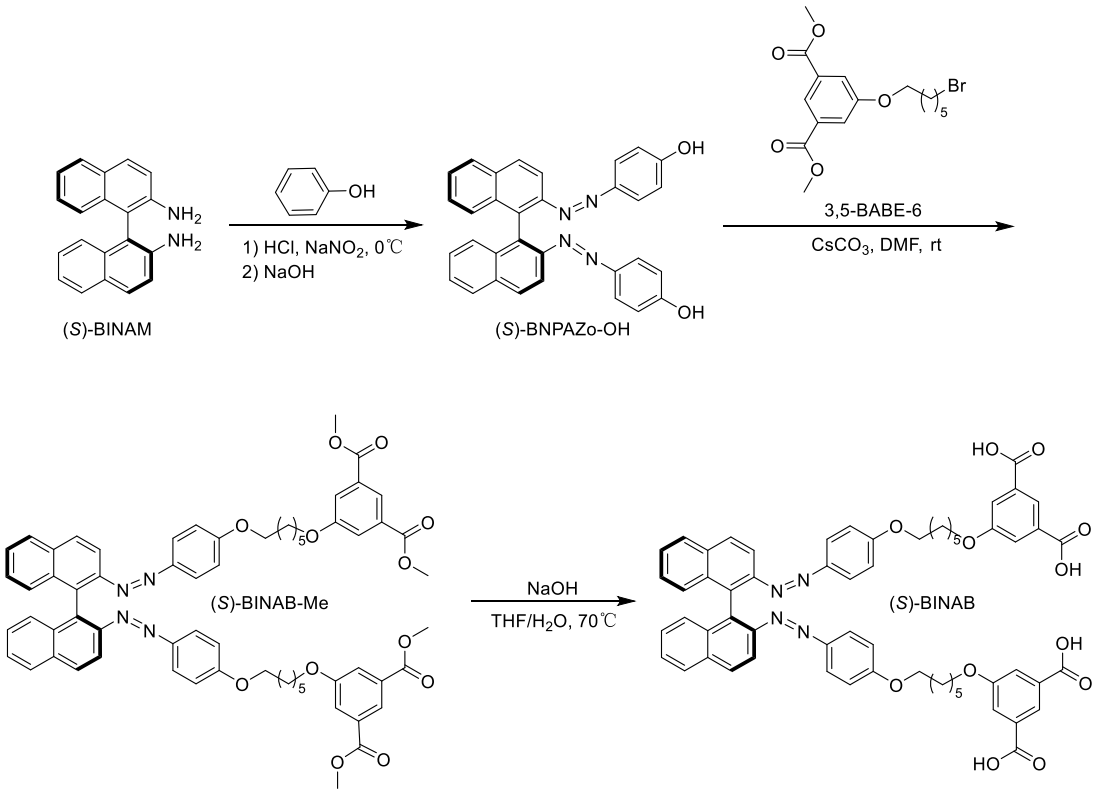

Scheme S1. Synthesis of (*S*)-BINAB.

Synthesis of (*S*)-BNPAZo-OH

(*S*)-[1,1'-binaphthalene]-2,2'-diamine ((*S*)-BINAM, 0.50 g, 1.76 mmol) was dissolved in a 3 M HCl aqueous solution, and a solution of sodium nitrite (0.29 g, 4.22 mmol) in H_2O (5 mL) was added dropwise under an ice bath. The resulted brownish-yellow suspension was added dropwise into a solution of phenol (0.36 g, 3.87 mmol) and NaOH (0.45 g, 11.25 mmol) in H_2O (7.5 mL) and reacted at room temperature for 4 h. The reaction mixture was extracted with dichloromethane (30 mL × 3) and washed with water (30 mL × 3). The collected organic layer was dried over Na_2SO_4 and concentrated under reduced pressure. The crude product was purified by silica gel column chromatography (silica gel, eluent: hexane/ethyl acetate = 10:1, v/v) to give (*S*)-BNPAZo-OH as an orange solid in 60% yield (0.53 g).

^{1}H NMR (400 MHz, DMSO-d_6) δ 10.17 (s, 2H), 8.19 (d, J = 9.0 Hz, 2H), 8.12 (d, J = 8.0 Hz, 2H), 8.07 (d, J = 9.0 Hz, 2H), 7.61 - 7.53 (t, 2H), 7.36 (t, J = 7.6 Hz, 2H), 7.25 (d, J = 8.4 Hz, 2H), 7.16 (d, J = 8.9 Hz, 4H), 6.70 – 6.65 (m, 4H).

^{13}C NMR (100 MHz, DMSO-d_6) δ 160.72, 147.77, 145.50, 135.62, 133.74, 133.53, 129.27, 128.41, 127.28, 127.12, 126.88, 124.40, 115.78, 114.22, 54.98.

HRMS (ESI-IT-TOF) m/z: $[M+Na]^+$ calcd for $C_{32}H_{22}N_4NaO_2^+$: 517.1635; found: 517.1607.

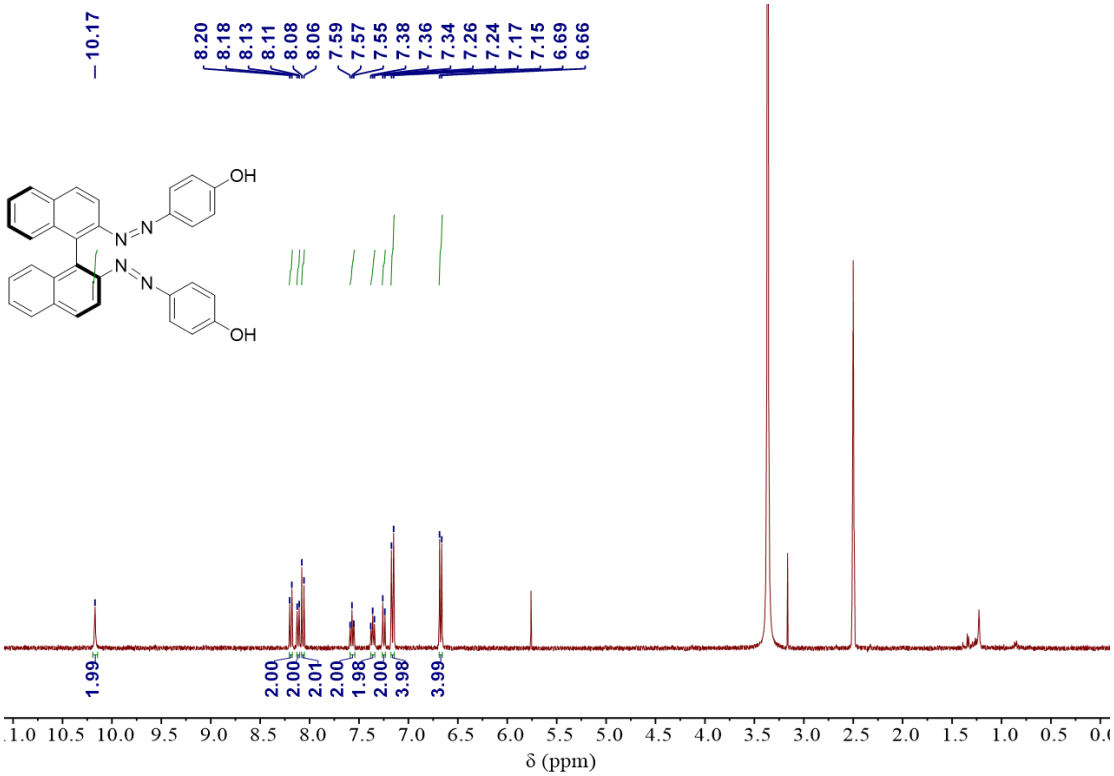

Fig. S1 ^{1}H NMR spectrum of (*S*)-BNPAZo-OH (400 MHz, DMSO-d_6).

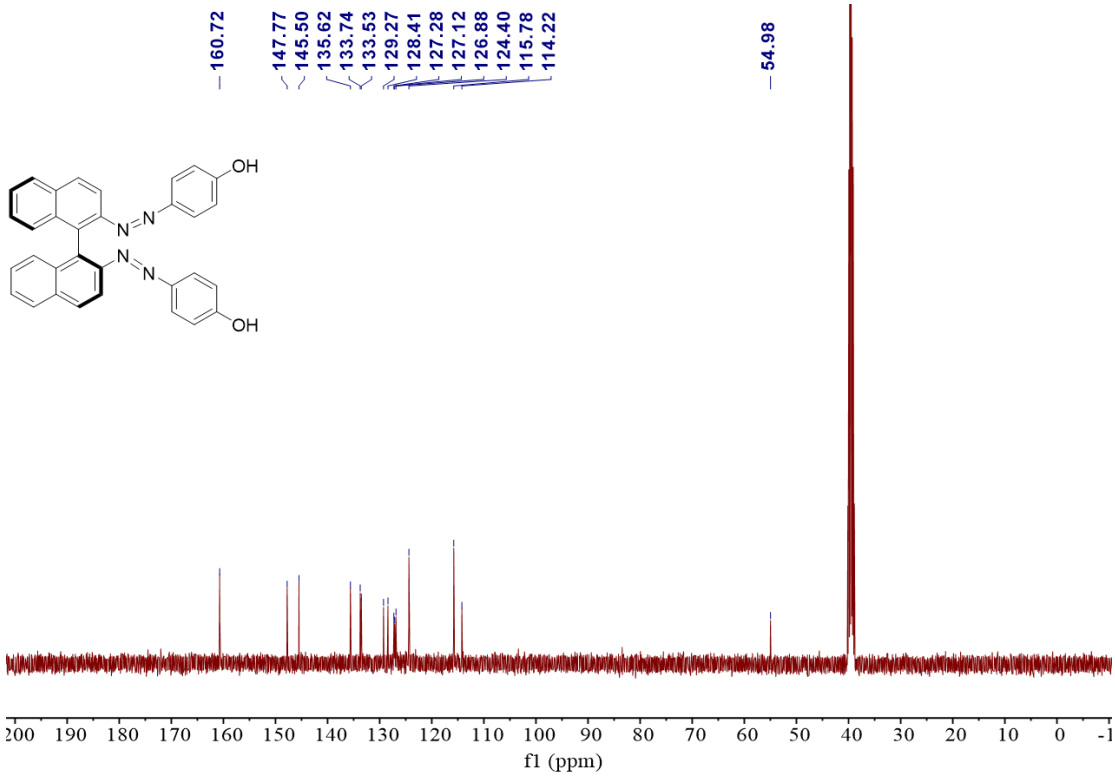

Fig. S2 ^{13}C NMR spectrum of (*S*)-BNPAZo-OH (100 MHz, DMSO-d_6).

ESI+

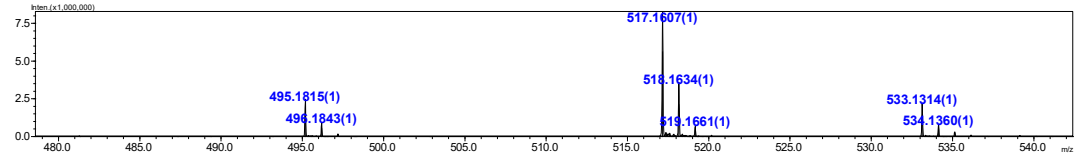

Fig. S3 HRMS of (*S*)-BNPAZo-OH (ESI+).

Synthesis of 3,5-BABE-6

A mixture of methyl 5-hydroxyisophthalate (2.00 g, 9.57 mmol) in anhydrous acetonitrile (60 mL) and anhydrous DMF (4 mL) was heated until complete dissolution. To the stirred solution was added 1,6-dibromohexane (19.2 mmol) and K_2CO_3 (1.40 g). The reaction mixture was refluxed at 88 °C for 12 h, then cooled to room temperature. The mixture was extracted with DCM (3 × 30 mL), and the combined organic layers were concentrated under reduced pressure. Purification by column chromatography afforded the product as a white solid in 65% yield.

^{1}H NMR (400 MHz, Chloroform-*d*) δ 8.25 (s, 1H), 7.72 (d, *J* = 1.4 Hz, 2H), 4.03 (t, *J* = 6.4 Hz, 2H), 3.93 (s, 6H), 3.42 (t, *J* = 6.8 Hz, 2H), 1.92 – 1.87 (m, 2H), 1.82 (dd, *J* = 8.5, 5.1 Hz, 2H), 1.52 (q, *J* = 3.6 Hz, 4H).

^{13}C NMR (100 MHz, Chloroform-*d*) δ 165.91, 158.93, 131.51, 122.60, 119.56, 68.13, 52.20, 33.54, 32.61, 28.75, 27.70, 25.04.

HRMS (ESI-IT-TOF) m/z: $[M+Na]^+$ calcd for $C_{16}H_{21}BrNaO_5^+$: 395.0456; found: 395.0475.

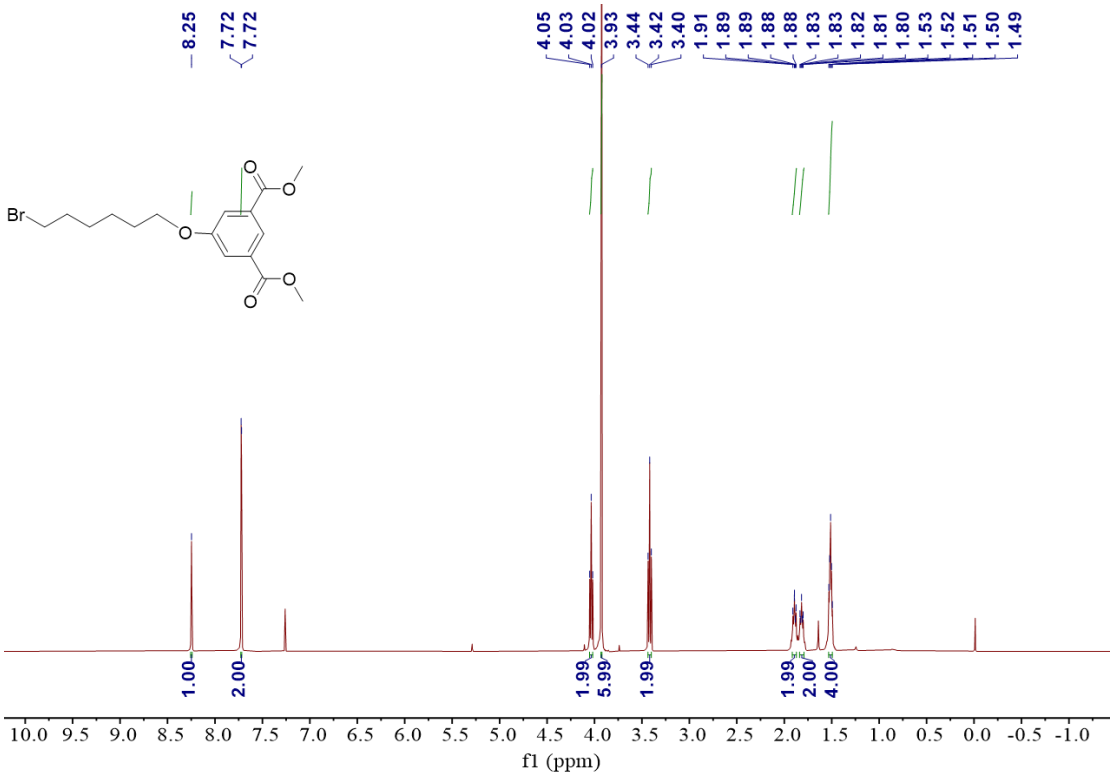

Fig. S4 ^{1}H NMR spectrum of 3,5-BABE-6 (400 MHz, Chloroform-*d*).

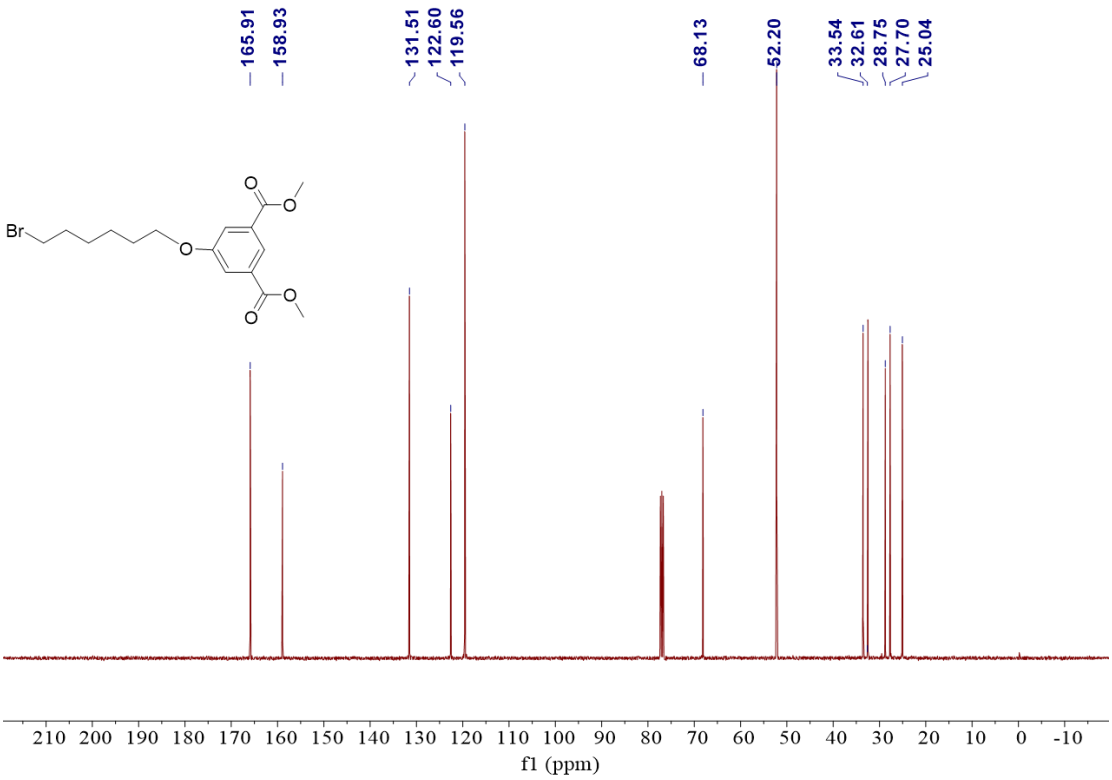

Fig. S5 ^{13}C-NMR spectrum of 3,5-BABE-6 (100 MHz, Chloroform-*d*).

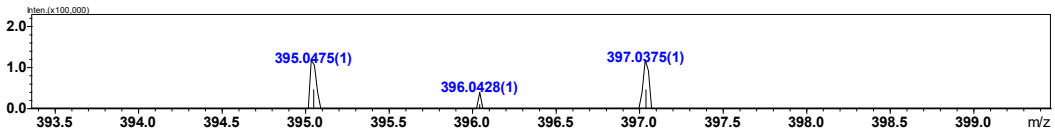

Fig. S6 HRMS of 3,5-BABE-6 (ESI$^+$).

Synthesis of (*S*)-BINAB-Me

Compound (*S*)-BNPAZo-OH (100 mg, 0.2 mmol) and 3,5-BABE-6 (0.43 mmol) were dissolved in anhydrous DMF (3 mL). Cesium carbonate (Cs_2CO_3, 145 mg, 0.45 mmol) was added, and the reaction mixture was stirred at room temperature for 5 h, with the progress monitored by TLC. Upon completion, the solvent was removed under reduced pressure. The residue was partitioned between dichloromethane (DCM) and water. The organic layer was separated, dried over anhydrous sodium sulfate (Na_2SO_4), and concentrated in vacuo. Purification by column chromatography on silica gel afforded the target compound (*S*)-BINAB-Me-n in 60% yield.

^{1}H NMR (400 MHz, Chloroform-*d*) δ 8.26 (s, 2H), 8.15 (d, *J* = 8.9 Hz, 2H), 8.04 (d, *J* = 9.0 Hz, 2H), 7.96 (d, *J* = 8.2 Hz, 2H), 7.72 (s, 4H), 7.49 (d, *J* = 6.7 Hz, 2H), 7.43 (s, 2H), 7.30 (d, *J* = 9.0 Hz, 4H), 7.24 (s, 2H), 6.71 (d, *J* = 8.2 Hz, 4H), 4.02 (t, *J* = 6.3 Hz, 4H), 3.93 – 3.89 (m, 16H), 1.78 (dt, *J* = 19.8, 6.5 Hz, 8H), 1.52 – 1.46 (m, 8H).

^{13}C NMR (100 MHz, Chloroform-*d*) δ 166.16, 161.10, 159.11, 148.26, 147.19, 136.63, 134.25, 134.14, 131.65, 128.91, 127.98, 127.77, 126.85, 126.50, 124.54, 122.77, 119.76, 114.39, 114.35,

68.34, 67.91, 52.37, 28.99, 28.94, 25.70.

HRMS (ESI-IT-TOF) m/z: $[M+Na]^+$ calcd for $C_{64}H_{62}N_4NaO_{12}^+$: 1101.4257; found: 1101.4262.

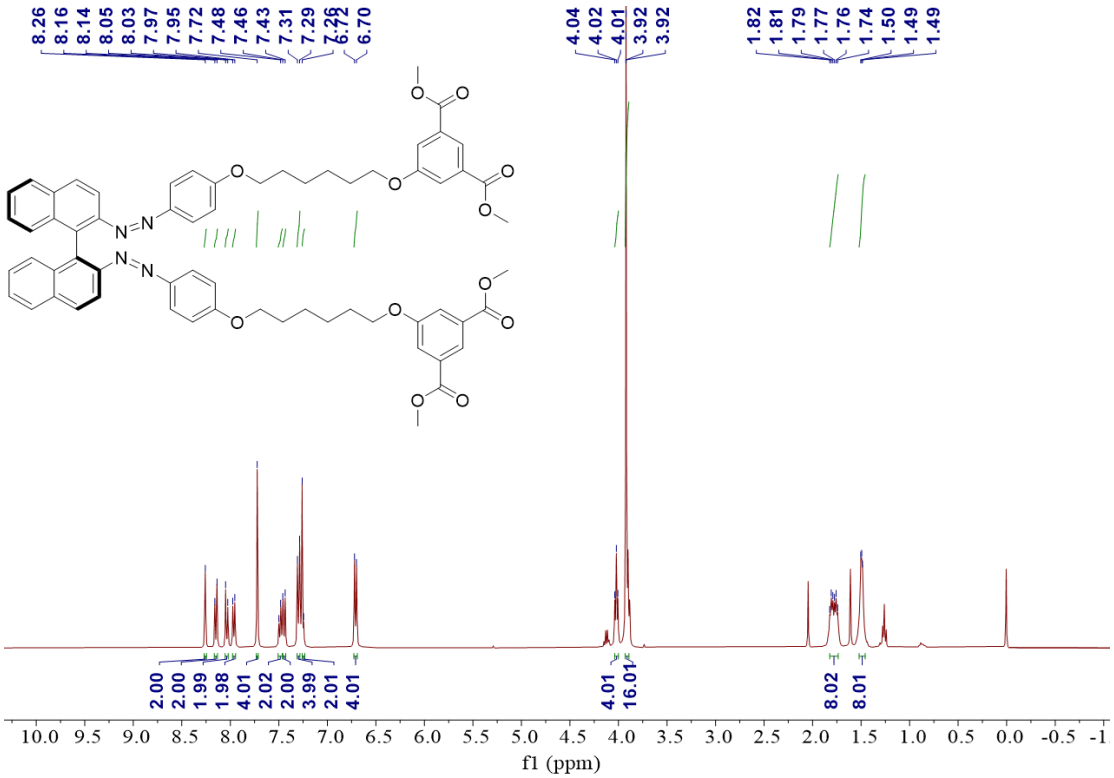

Fig. S7 ^{1}H NMR spectrum of (*S*)-BINAB-Me (400 MHz, Chloroform-*d*).

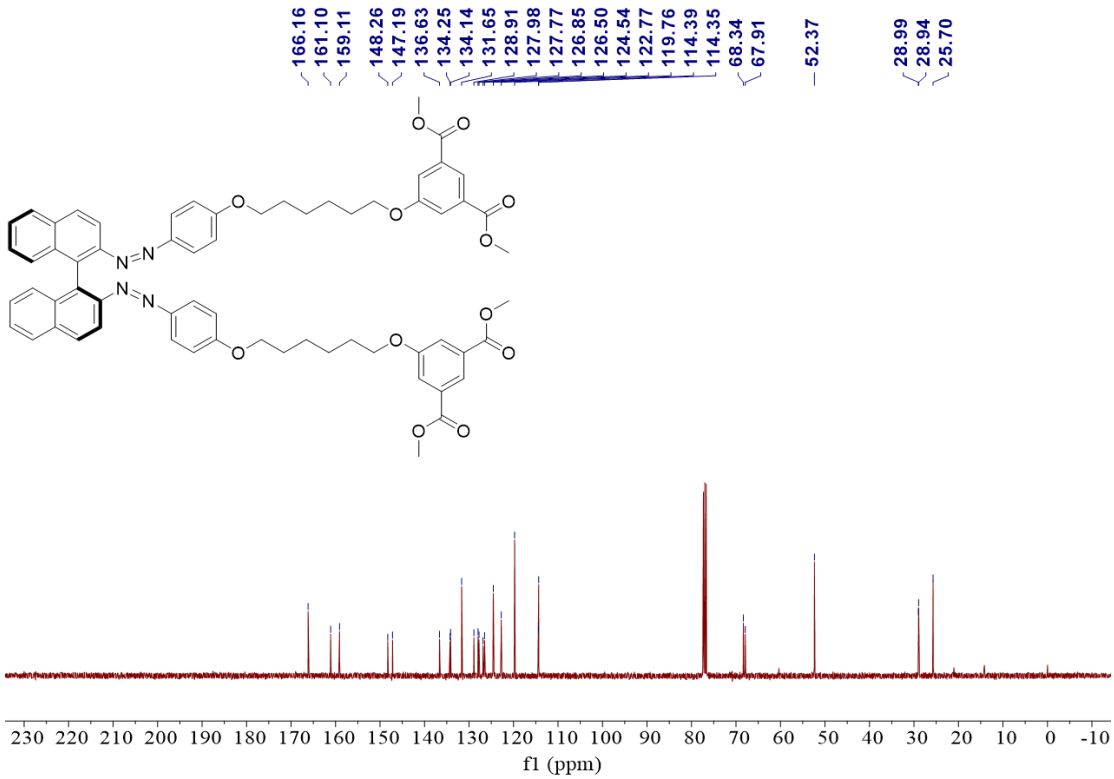

Fig. S8 ^{13}C NMR spectrum of (*S*)-BINAB-Me (100 MHz, Chloroform-*d*).

ESI$^+$

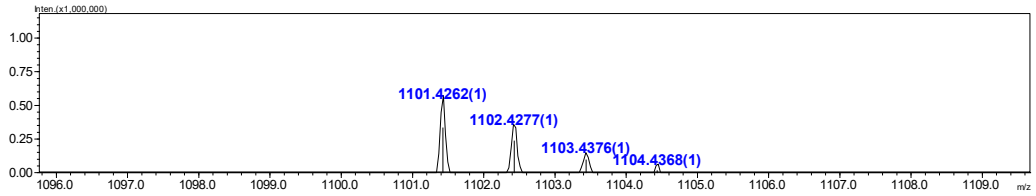

Fig. S9 HRMS spectra of (*S*)-BINAB-Me (ESI$^+$).

Synthesis of (*S*)-BINAB

(*S*)-BINAB-Me was dissolved in THF, followed by the addition of an aqueous NaOH solution. The mixture was stirred at 70 °C for 3 h. After cooling to room temperature, the pH was adjusted to 1 with hydrochloric acid. The solvent was removed under reduced pressure, and the residue was extracted with ethyl acetate (EA) and water. The organic layer was dried over anhydrous Na_2SO_4, filtered, and concentrated in vacuo to afford an orange solid powder in 88% yield.

^{1}H NMR (400 MHz, DMSO-d_6) δ 13.22 (s, 4H), 8.19 (d, J = 9.1 Hz, 2H), 8.11 (d, J = 8.1 Hz, 2H), 8.08 (d, J = 11.8 Hz, 4H), 7.61 (d, J = 1.4 Hz, 4H), 7.57 (t, J = 7.5 Hz, 2H), 7.36 (t, J = 7.6 Hz, 2H), 7.28 (d, J = 8.4 Hz, 2H), 7.23 (d, J = 9.0 Hz, 4H), 6.85 (d, J = 9.1 Hz, 4H), 4.03 (t, J = 6.4 Hz, 4H), 3.92 (t, J = 6.5 Hz, 4H), 1.68 (dt, J = 18.4, 6.5 Hz, 8H), 1.44 – 1.37 (m, 8H).

^{13}C NMR (100 MHz, DMSO-d_6) δ 166.44, 161.23, 158.80, 147.74, 146.30, 135.87, 133.83, 133.48, 132.58, 129.34, 128.41, 127.40, 127.16, 126.90, 124.05, 122.12, 119.01, 114.88, 114.11, 68.00, 67.84, 28.43, 25.13.

HRMS (ESI-IT-TOF) m/z: [M+H$^+$] calcd for $C_{60}H_{55}N_4O_{12}^+$: 1023.3811; found: 1023.3808.

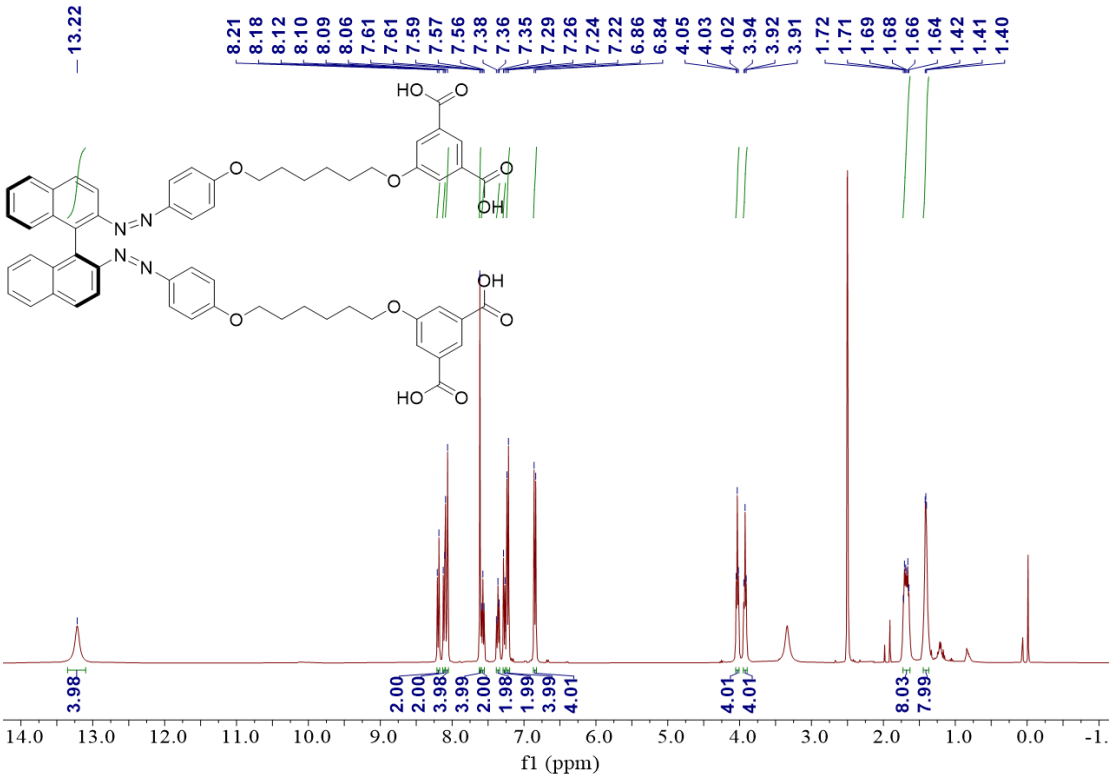

Fig. S10 ^{1}H NMR spectrum of (*S*)-BINAB (400 MHz, DMSO-d_6).

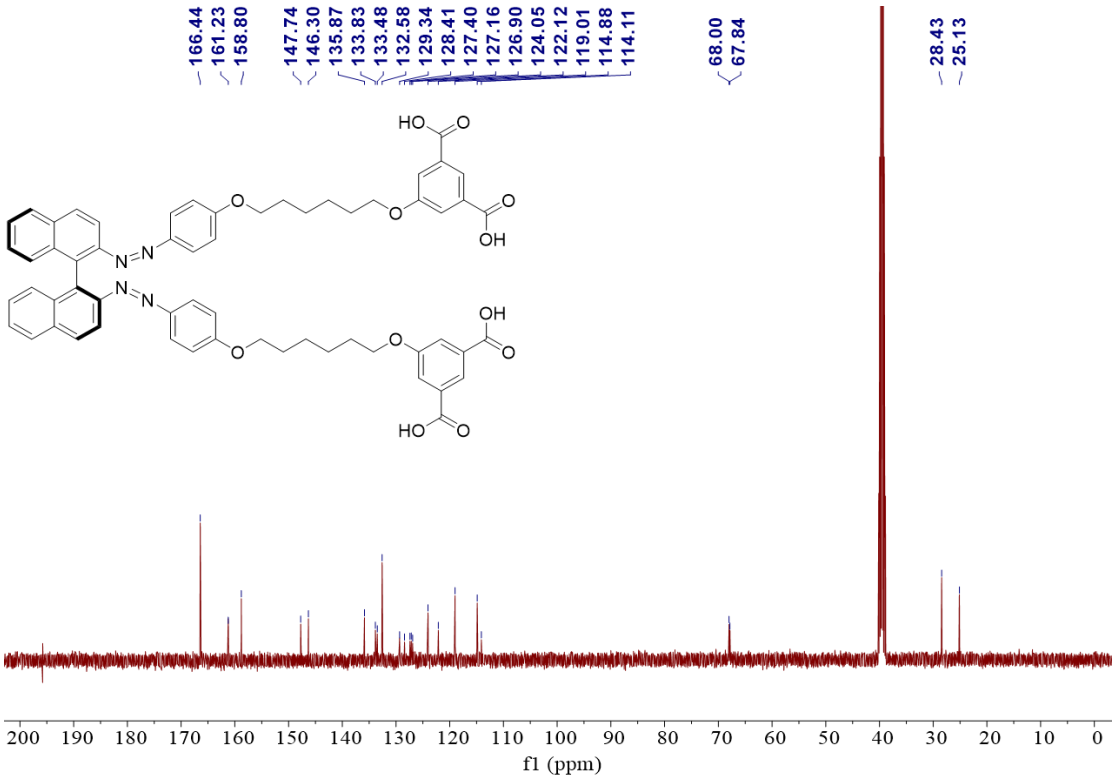

Fig. S11 ^{13}C NMR spectrum of (*S*)-BINAB (100 MHz, DMSO-d_6).

ESI$^+$

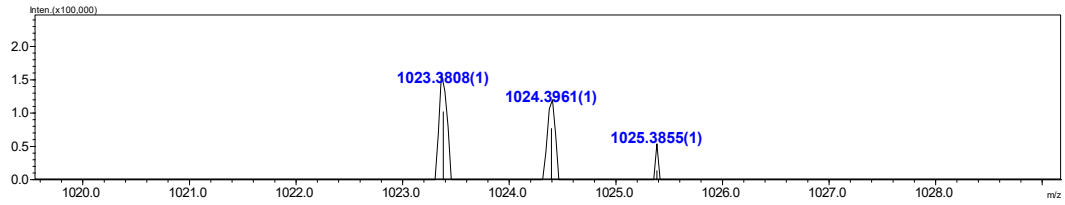

Fig. S12 HRMS spectra of (*S*)-BINAB (ESI$^+$).

The synthesis method for (*R*)-BINAB is the same as for (*S*)-BINAB, except that (*S*)-BINAM is replaced with (*R*)-BINAM.

^{1}H NMR (400 MHz, DMSO-d_6) δ 8.19 (d, J = 9.1 Hz, 2H), 8.11 (d, J = 8.6 Hz, 2H), 8.08 (d, J = 10.5 Hz, 4H), 7.61 (d, J = 1.4 Hz, 4H), 7.57 (t, J = 7.3 Hz, 2H), 7.36 (t, J = 7.8 Hz, 2H), 7.27 (d, J = 8.4 Hz, 2H), 7.22 (d, J = 8.7 Hz, 4H), 6.84 (d, J = 8.7 Hz, 4H), 4.03 (t, J = 6.4 Hz, 4H), 3.92 (t, J = 6.5 Hz, 4H), 1.74 – 1.62 (m, 8H), 1.41 (s, 8H).

^{13}C NMR (100 MHz, DMSO-d_6) δ 166.45, 161.23, 158.80, 147.75, 146.31, 135.87, 133.83, 133.49, 132.59, 129.34, 128.41, 127.40, 127.15, 126.91, 124.05, 122.12, 119.02, 114.88, 114.12, 68.01, 67.84, 28.43, 25.13.

HRMS (ESI-IT-TOF) m/z: [M+H$^+$] calcd for $C_{60}H_{55}N_4NaO_{12}^+$: 1045.3631; found: 1045.3628.

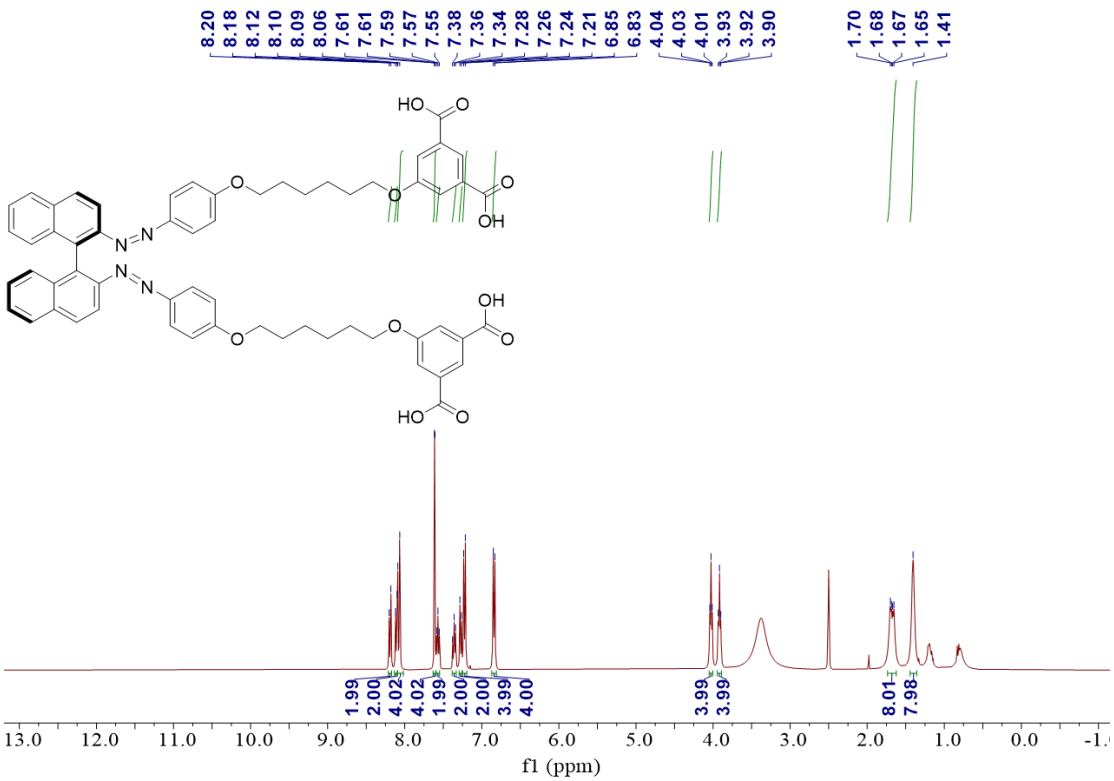

Fig. S13 ^{1}H NMR spectrum of (*R*)-BINAB (400 MHz, DMSO-d_6).

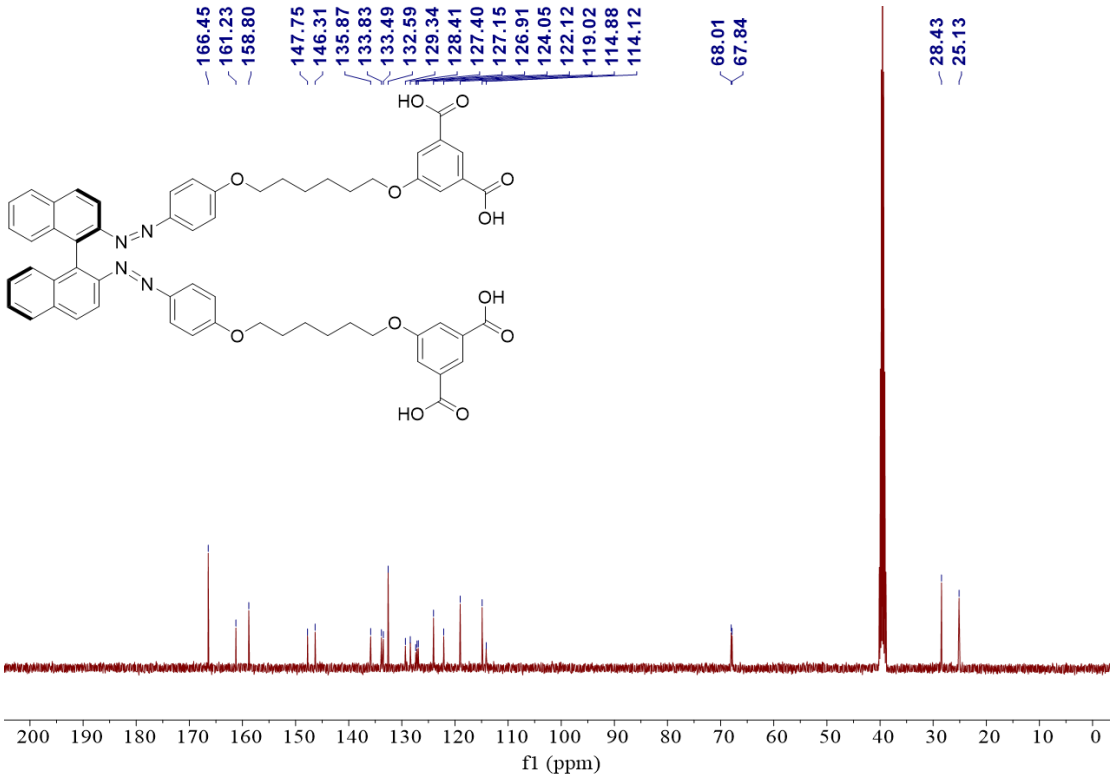

Fig. S14 ^{13}C NMR spectrum of (*R*)-BINAB (100 MHz, DMSO-d_6).

ESI$^+$

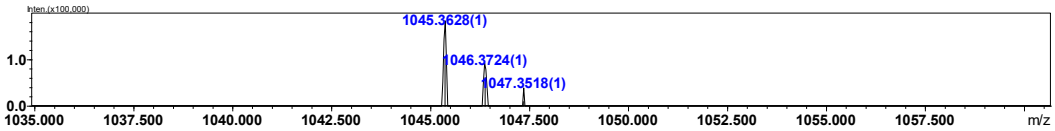

Fig. S15 HRMS spectra of (*R*)-BINAB (ESI$^+$).

2. Supplementary Figures and Tables

Table S1. Gelation properties of (*S*)-BINAB. [(*S*)-BINAB] = 10 mM[a].

Solvent	Result	Solvent	Result	Solvent	Result
CH_3CN	I	Acetone	S	THF	S
$CHCl_3$	I	Cy	S	Acetone/H_2O	P
H_2O	I	DMSO	S	AcOH/H_2O	P
CH_2Cl_2	I	DMF	S	DMF/H_2O	P
EG	I	1,4-Dioxane	S	DMSO/H_2O	S
hexane	I	EtOH	S	EtOH/H_2O	PG
MCH	I	$(CH_3CH_2)_2O$	S	MeOH/H_2O	PG
Toluene	I	i-PrOH	S	THF/H_2O	PG
CH_3COOH	S	Methanol	S	i-PrOH/H_2O (1/1, v/v)	G (8.0 mM)

[a] I: insoluble, G: stable gel, PG: partial gel, S: sol, P: precipitate. In parentheses, the critical gelation concentration (CGC) and the volume ratio of organic solvent and water required to form stable water-induced gels, respectively, are given (Test concentration: 10 mM).

Fig. S16 Gelation properties of (*S*)-BINAB in different solvents mixed with water (1:1, v/v) ([(*S*)-BINAB] = 8 mM)

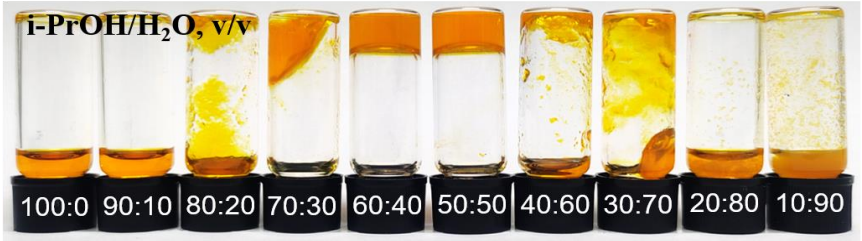

Fig. S17 Impact of varying water content on the gel formation of (*S*)-BINAB in i-PrOH/H_2O. The images show, from left to right, a gradual increase in the water fraction (f_w) from 0% to 100%.

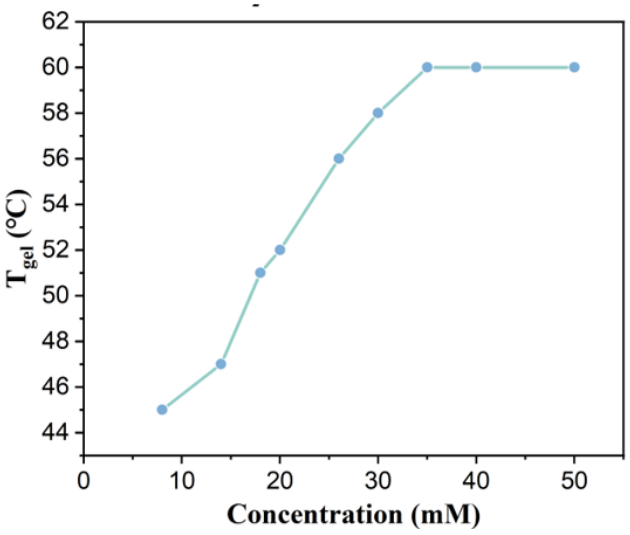

Fig. S18 Macroscopic phase transition temperature of the (*S*)-BINAB gel.

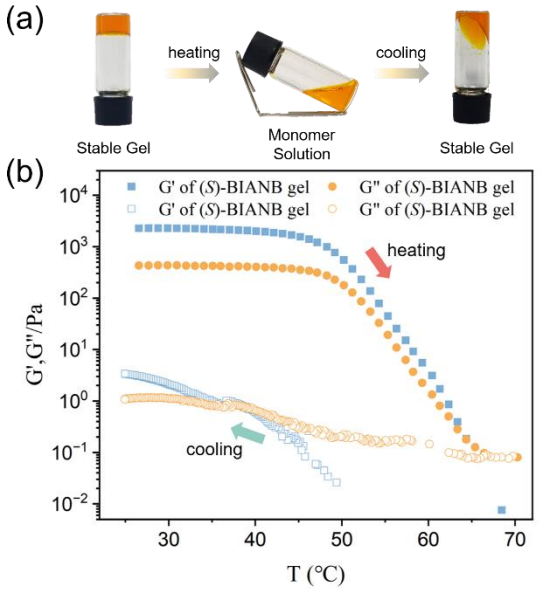

Fig. S19 (a) Macroscopic thermoreversibility of (*S*)-BINAB gel. (b) The temperature-sweep rheological measurements over one heating-cooling cycle of (*S*)-BINAB gel.

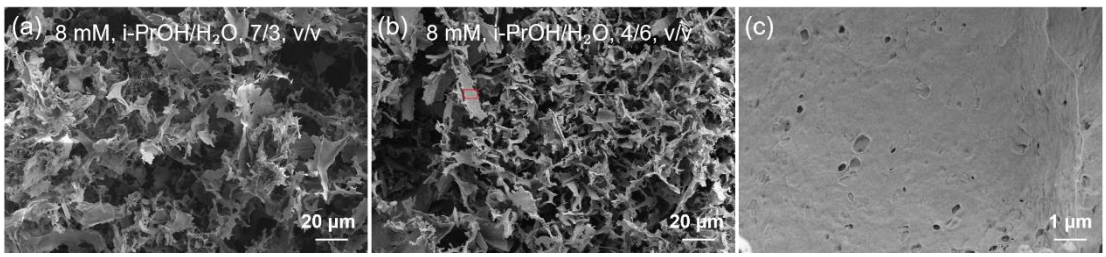

Fig. S20 SEM images of partial gel formed by (*S*)-BINAB. (a) SEM image of the partial gel prepared at 8 mM in i-PrOH/H_2O (7:3, v/v). (b) SEM image of the partial gel prepared at 8 mM in i-PrOH/H_2O (4:6, v/v). (c) Magnified SEM image of the lamellar aggregate surface (region marked by red box in panel b).

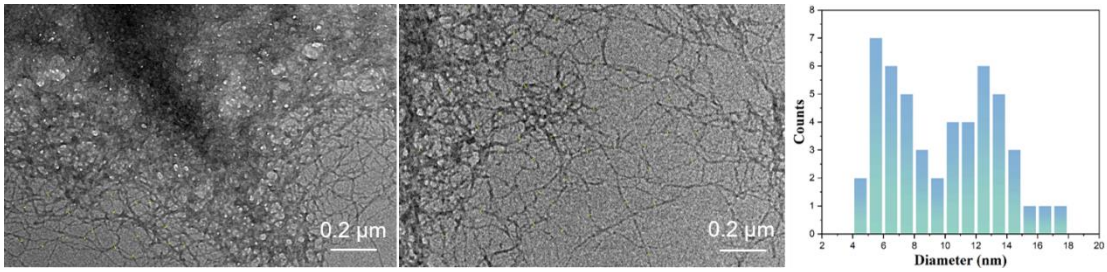

Fig. S21 Transmission electron microscopy (TEM) of the (*S*)-BINAB gel and fiber diameter measurement and statistical analysis.

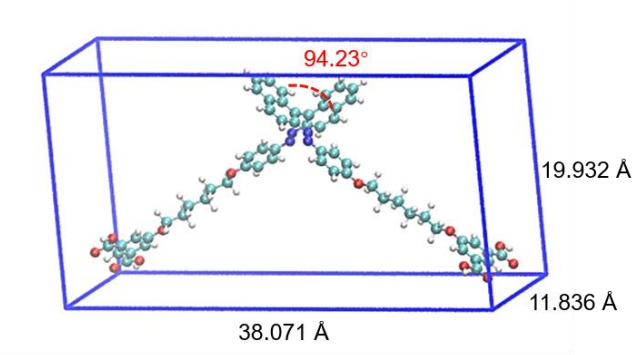

Fig. S22 Energy-minimum optimized structure of (*S*)-BINAB by DFT computation at B3LYP-D3(BJ)/6-311+G(d,p) level. The length, width, and height of (*S*)-BINAB were calculated by the Multiwfn program. The solid balls represent carbon (cyan), hydrogen (white), nitrogen (blue), and oxygen (red).

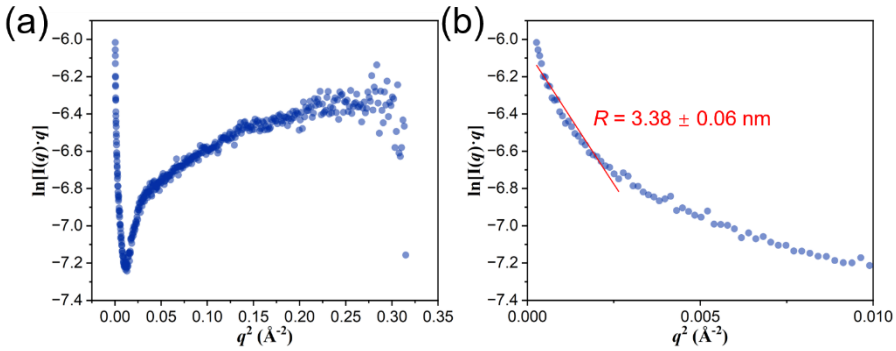

Fig. S23 (a) SAXS profile of the (*S*)-BINAB gel presented as a plot of ln(I(q)·q) vs. q^2. (b) The linear fit (red line) to the low-q^2 region yields a slope of -285.22, corresponding to a cross-sectional radius of R = 3.38 ± 0.06 nm for the fibrous assemblies.

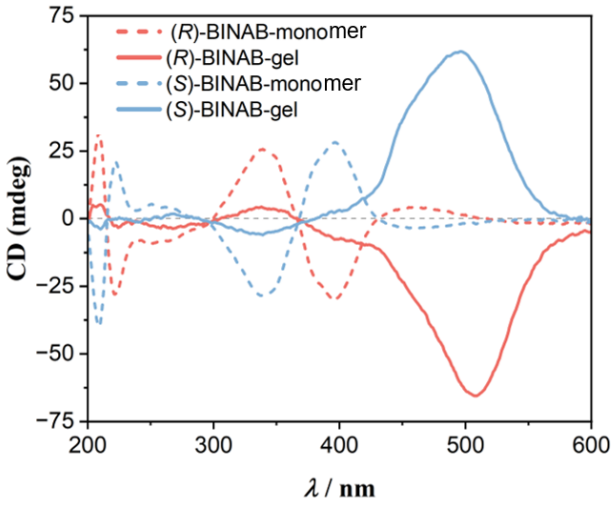

Fig. S24 CD spectra of the (*S*)- and (*R*)-BINAB monomers and their respective gel states.

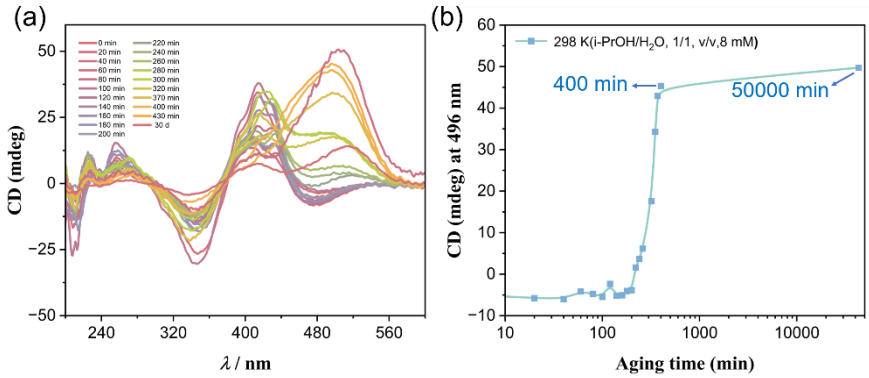

Fig. S25 (a) CD spectra of (*S*)-BINAB gel against aging time. (b) Change in CD signal intensity of (*S*)-BINAB gel at 496 nm as a function of aging time ([(*S*)-BINAB] = 8 mM).

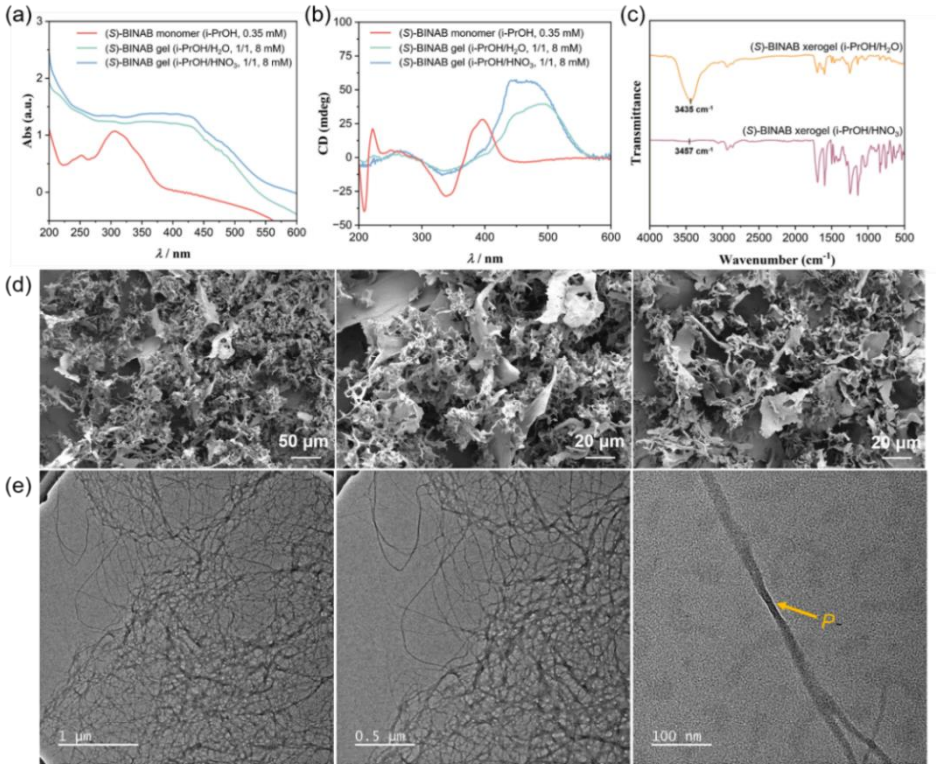

Fig. S26 (a) UV-Vis spectra of (*S*)-BINAB monomer, (*S*)-BINAB gel (i-PrOH/H_2O, 1:1, v/v, 8 mM) and (*S*)-BINAB gel (i-PrOH/13.5 mM HNO_3 (pH = 1.9) mixture (1:1, v/v), 8 mM). (b) CD spectra of (*S*)-BINAB monomer, (*S*)-BINAB gel (i-PrOH/H_2O, 1:1, v/v, 8 mM) and (*S*)-BINAB gel (i-PrOH/13.5 mM HNO_3 (pH = 1.9) mixture (1:1, v/v), 8 mM). (c) FT-IR spectra of (*S*)-BINAB gel (i-PrOH/H_2O, 1:1, v/v, 8 mM) and (*S*)-BINAB gel (i-PrOH/13.5 mM HNO_3 (pH = 1.9) mixture (1:1, v/v), 8 mM). (d) SEM image of the (*S*)-BINAB gel formed under acidic conditions (i-PrOH/13.5 mM HNO_3 (pH = 1.9) mixture (1:1, v/v), 8 mM). (e) TEM image of the (*S*)-BINAB gel formed under acidic conditions (i-PrOH/13.5 mM HNO_3 (pH = 1.9) mixture (1:1, v/v), 8 mM).

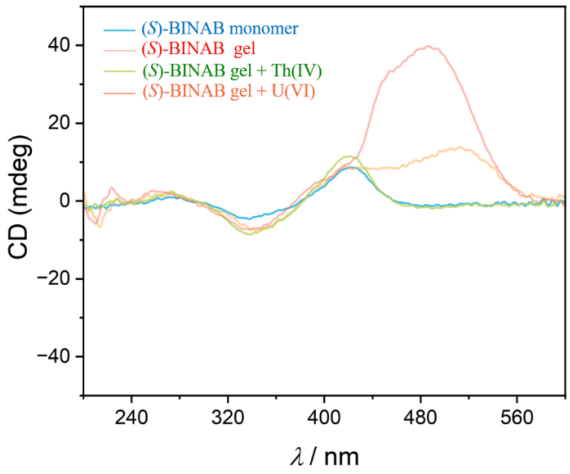

Fig. S27 Circular dichroism (CD) spectra of (*S*)-BINAB (3 mM in i-PrOH/13.5 mM HNO_3 (pH = 1.9) mixture (1:1, v/v)) were recorded after a 10 minute incubation following the addition of 1.0 equivalent of Th^{4+} or UO_2^{2+}.

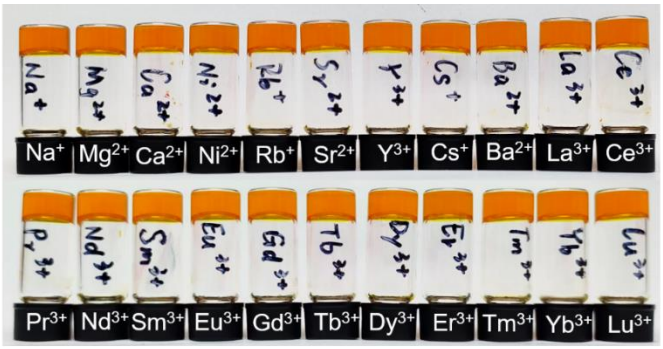

Fig. S28 Inverted vials containing (*S*)-BINAB gel (3 mM in i-PrOH/13.5 mM HNO_3 (pH = 1.9) mixture (1:1, v/v)) with 20 equivalents of other metal ions (except for $Th^{4+}$and UO_2^{2+}).

Fig. S29 (a) The effect of adding different equivalents of Th^{4+} to a 3 mM (*S*)-BINAB solution in i-PrOH/13.5 mM HNO_3 (pH = 1.9) mixture (1:1, v/v) (b) The effect of adding different equivalents UO_2^{2+} to 3 mM (*S*)-BINAB in i-PrOH/13.5 mM HNO_3 (pH = 1.9) mixture (1:1, v/v) (The numbers at the bottom represent the equivalents of Th^{4+} or UO_2^{2+} ions).

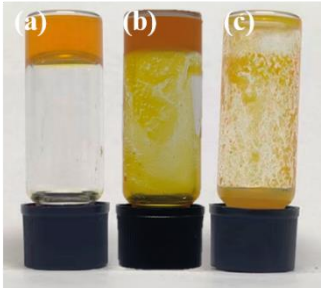

Fig. S30 Anti-interference ability of the BINAB gel in Th^{4+} recognition. (a) (*S*)-BINAB hydrogel without any metal ions (3.0 mM in i-PrOH/13.5 mM HNO_3 (pH = 1.9) mixture (1:1, v/v)). (b) (*S*)-BINAB treated with a mixture of other metal ions (2 equiv. per ion, without UO_2^{2+}). (c) (*S*)-BINAB gel in the presence of other metal ions and Th^{4+} (0.1 equiv. of Th^{4+} with 2 equiv. of each competing ion (without UO_2^{2+})).

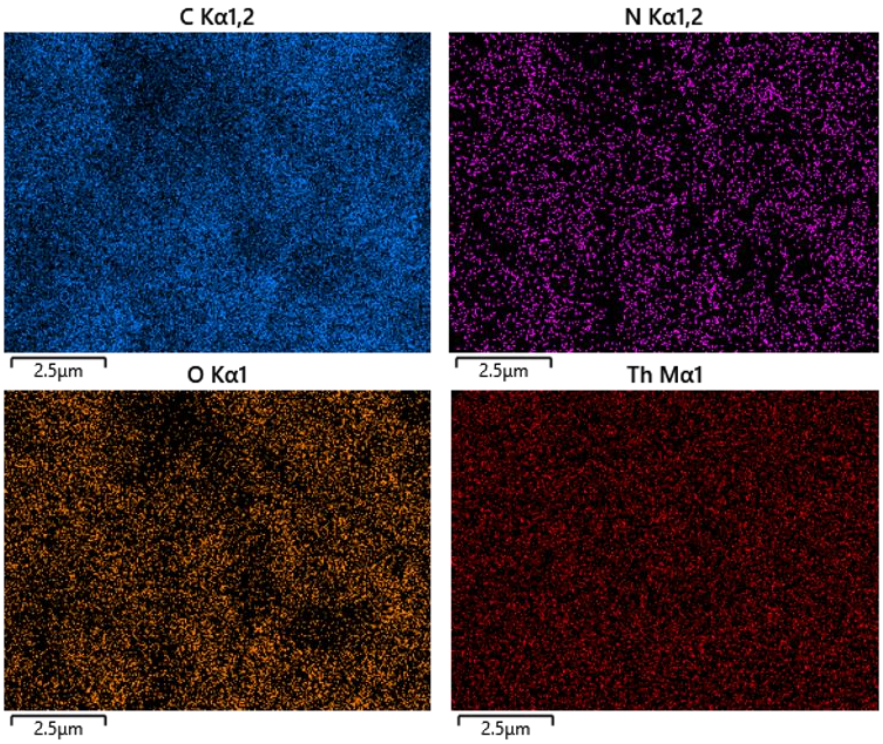

Fig. S31 Elemental mapping of the (*S*)-BINAB thorium complex obtained by EDS.

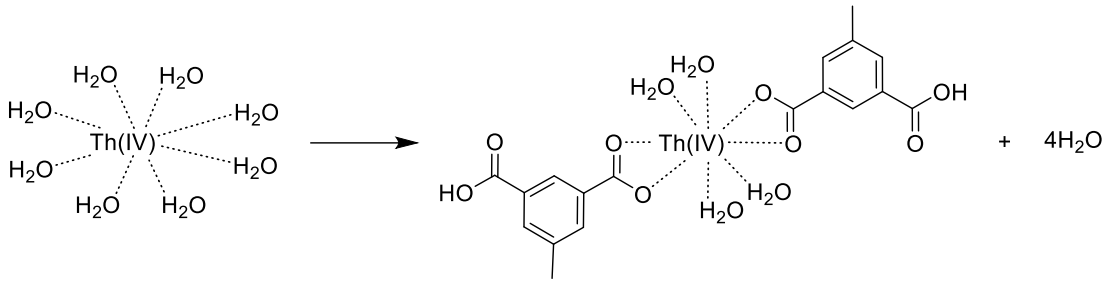

Fig. S32 Schematic diagram of the proposed coordination mode of (*S*)-BINAB with Th(IV).